

# Communication

## EMSIW-Based Compact High Gain Wide Full Space Scanning LWA With Improved Broadside Radiation Profile

Anirban Sarkar<sup>1b</sup>, Abhishek Sharma, Animesh Biswas<sup>1b</sup>, and M. Jaleel Akhtar<sup>1b</sup>

**Abstract**—A novel compact high gain eighth-mode substrate-integrated-waveguide (EMSIW)-based double asymmetry (DA) composite right/left-handed (CRLH) leaky-wave antenna with larger degrees of freedom to control the efficiency is proposed and investigated. The proposed tilted DA radiating EMSIW incorporated with radiating interdigital capacitive (IDC) slots enables the unit cell to hold CRLH property with improved compactness and gain. The DA not only provides increased efficiency at broadside frequency than off-broadside but also offers more degrees of freedom to independently control the series and shunt resonators of the proposed geometry. Dispersion analysis is done by full-wave simulation and validated by theoretical analysis through predicted equivalent circuit model for achieving the balance condition of the unit cell which facilitates the complete elimination of open-stopband. Due to the systematic placement of interdigital slots on radiating EMSIW unit cell, the radiation intensity profile is significantly enhanced, which leads to higher directivity and notably enhanced gain (17.96 dBi). The proposed prototype is  $5\lambda_0$  long having ten unit cells. The beam scanning range of the proposed antenna is  $107^\circ$  within 9–13.5 GHz, with the maximum broadside radiation efficiency of  $\sim 96\%$ .

**Index Terms**—Composite right/left-handed (CRLH), leaky-wave antenna (LWA), substrate-integrated waveguide (SIW).

### I. INTRODUCTION

Composite right/left-handed (CRLH) transmission lines (TLs) represent an artificially structured media having unique properties which have been used extensively in several applications over the past decades [1]. In addition to this, with the rapid growth of wireless technology, the demand for improved antenna performances such as high gain, larger scanning range, etc., is highly needed in various surveillance systems and many scanning applications. Leaky-wave antenna (LWA) appears to be an appropriate choice for such applications, which belongs to a traveling wave antenna family and has the capability of frequency beam scanning [2]. Recently, several compact LWAs based on microstrip as well as on substrate-integrated waveguide (SIW) environment open a new avenue for frequency-scanning antenna design [3]–[5].

Usually, the microstrip- and waveguide-based LWAs restrict the broadside radiation, except the periodic LWAs having spatial harmonic and complex feeding network. Balanced CRLH TLs are one of the best choices to achieve broadside radiation which is capable of eliminating the open-stopband between the left-handed (LH) and right-handed (RH) regions. In the past, several CRLH-based LWAs have been developed for backfire to endfire radiation, including broadside [6], [7]. Over the last few years, the use of half-mode SIW (HMSIW) and quarter-mode SIW (QMSIW) in designing compact antennas, as well as frequency beam-scanning antennas, has also increased extensively [8]–[12]. However, it is very difficult to achieve higher efficiency at broadside frequency, a constant high

gain over the full operating frequency band maintaining a fair scanning range, design simplicity, and compactness. In [13] and [14], a new technique of efficiency enhancement at broadside frequency ( $\eta_{f_0}$ ) has been proposed by using transversal asymmetry (TA) and double asymmetry (DA), respectively. However, both these designs suffer from drawbacks such as larger electrical size, lower gain, and higher cross-polar level. In this communication, a novel DA radiating structure integrated with the interdigital capacitive (IDC) slots has been proposed, which results into improved gain and higher efficiency as compared to those of earlier proposed simple DA structures [14]. It is to be noted that although the simple SIW-based LWAs having IDC slots have recently been proposed in [6] and [16]–[20], most of these designs either have the larger electrical size or lesser beam scanning range with the typical maximum radiation efficiency of lesser than 80%. Hence, it can be inferred that the proposed IDC slot integrated DA radiating structures resulting in higher overall gain, improved efficiency, and compact geometry are quite novel which have not been presented earlier in the literature.

In this communication, an electrically small eighth-mode SIW (EMSIW) resonator incorporated with the interdigital slot is designed for the realization of compact high gain DA CRLH LWA for full-space scanning through broadside with increased broadside radiation efficiency. The proposed design provides much easier independent control over series and shunt resonators by tuning the tilt angle of the IDC slot ( $\theta$ ) and the EMSIW resonator ( $\zeta$ ), respectively, to achieve the balanced condition. This further helps to tune the transformation ratio (T) and enhances  $\eta_{f_0}$  notably. The performance of the proposed antenna is optimized using HFSS and validated by experiments. Due to the appropriate placement of IDC slots on the top of the radiating EMSIW resonator, the radiation intensity profile, gain, and  $\eta_{f_0}$  are improved without significantly increasing the length. The scanning angle can be varied from  $-64^\circ$  to  $+43^\circ$  by varying frequency from 9 to 13.5 GHz with the radiator length of  $5\lambda_0$ .

### II. PROPOSED DOUBLE ASYMMETRY CRLH UNIT CELL AND CIRCUIT ANALYSIS

First, the EMSIW is developed where a square SIW resonator is divided across the perfect open symmetry plane (fictitious magnetic wall) [15]. The EMSIW unit cell is slightly tilted at an angle  $\zeta$  with proper feeding line position, which controls the radiation characteristic as well as scanning range of the antenna. The normalized phase constant and attenuation constant are optimized with  $\zeta = 21^\circ$ ,  $m_1 = 2.36$  mm,  $L_1 = 8.51$  mm,  $m_2 = 2.32$  mm,  $d = 0.8$  mm, and  $s = 1.2$  mm. IDC slots are etched on the top of the radiating tilted EMSIW resonator to realize the novel CRLH media [Fig. 1(a)], which exhibits larger radiation intensity compared to the simple EMSIW or conventional series-fed patch based LWA [14] as shown in Fig. 2(a). Hence, this proposed unit cell provides higher directivity and gain. The radiation intensity in a particular direction is straightway defined as the radiated power from a radiating structure per unit solid angle. However, in HFSS simulator, the radiation intensity of the proposed unit cell is determined as

Manuscript received July 5, 2018; revised January 2, 2019; accepted May 9, 2019. Date of publication May 29, 2019; date of current version August 12, 2019. (Corresponding author: Anirban Sarkar.)

The authors are with the Department of Electrical Engineering, IIT Kanpur, Kanpur 208016, India (e-mail: anirban.skr227@gmail.com).

Color versions of one or more of the figures in this communication are available online at <http://ieeexplore.ieee.org>.

Digital Object Identifier 10.1109/TAP.2019.2918443

0018-926X © 2019 IEEE. Personal use is permitted, but republication/redistribution requires IEEE permission.

See [http://www.ieee.org/publications\\_standards/publications/rights/index.html](http://www.ieee.org/publications_standards/publications/rights/index.html) for more information.

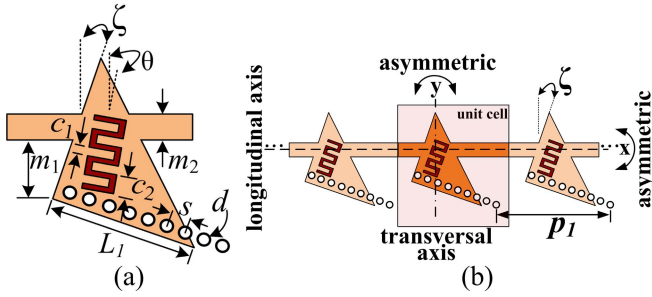


Fig. 1. (a) Proposed unit cell. (b) Layout of the proposed CRLH-based DA balanced LWA.

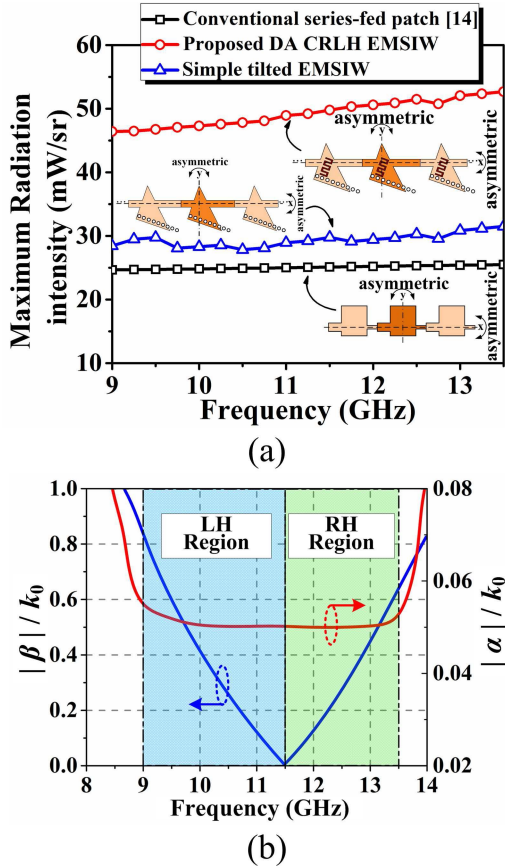


Fig. 2. (a) Comparison of radiation intensity per unit cell for conventional and proposed design. (b) Dispersion diagram of the balanced unit cell with  $c_1 = 0.26$  mm and  $c_2 = 0.84$  mm.

$U(\theta, \phi) = (|E|^2 r^2) / 2\eta_0$ , where  $|E|$  is the magnitude of the  $E$ -field,  $\eta_0$  is the intrinsic impedance in free space ( $376.7 \Omega$ ), and  $r$  is the distance from antenna in meters. Moreover, the CRLH unit cell exhibits DA with respect to transverse as well as a longitudinal axis as shown in Fig. 1(b), where the independent control over series and shunt resonators of the proposed unit cell to tune the transformation ratio is predominantly a unique feature of the proposed antenna to enhance the efficiency at broadside frequency. Generally, the use of interdigital slot on radiating EMSIW causes higher radiation loss per unit cell. Hence, the condition for  $\sim 90\%$  of total power will be radiated into space is fulfilled with the much compact radiator length of  $5\lambda_0$ . To the author's best knowledge, this feature is not utilized so far in the available literature. In full-wave optimization of unit-cell analysis, isolation of the series mode with PEC boundaries and shunt mode with perfect magnetic conductor boundaries is achieved from where the series resonance frequency ( $f_{se}$ ), the series radiation

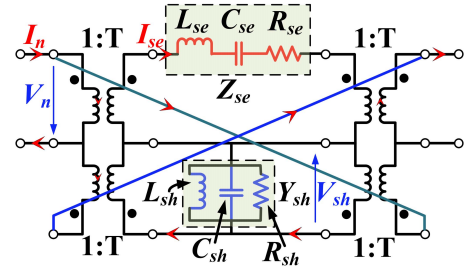


Fig. 3. Equivalent lattice circuit model of the proposed LWA unit cell.

efficiency ( $\eta_{se}$ ), the shunt resonance frequency ( $f_{sh}$ ), and the shunt radiation efficiency ( $\eta_{sh}$ ) are calculated [14].

#### A. Technique 1: Enhancement of $\eta_{f_0}$ by Independent Shunt Parameter Control Equivalently Varying EMSIW Resonator Tilt Angle ( $\zeta$ )

The equivalent circuit model of the proposed unit cell can be obtained by dividing the unit cell into the series and shunt resonators along with four coupling transformers having transformation ratio  $1:T$  which control the coupling of power ratios between series and shunt resonators. The input and output coupling sections are represented by two transformers having the transformation ratio  $1:T$ , as shown in Fig. 3. The series resonance is comprised of series inductance ( $L_{se}$ ) and series capacitance ( $C_{se}$ ) which are due to the presence of the top wall of the tilted EMSIW resonator and the tilted IDC slot, respectively. The shunt resonance is comprised of shunt inductance ( $L_{sh}$ ) and shunt capacitance ( $C_{sh}$ ) which are due to metallic vias and ground plane-tilted EMSIW resonator top surface, respectively. The parameter  $T$  can be physically interpreted as an additional variable which can be changed by varying the tilt angle of EMSIW resonator ( $\zeta$ ). The equivalent circuit lattice model of the unit cell is shown below in Fig. 3. The circuit simulations are performed in advanced design system (ADS). Primarily,  $f_{se}$  and  $f_{sh}$  are calculated by imposing the odd excitation with  $Im\{Z_{se}\}|_{f_{se}} = 0$  and even excitation with  $Im\{Y_{sh}\}|_{f_{sh}} = 0$ , respectively. If we vary the EMSIW resonator tilt angle  $\zeta$ , the affected parameters are  $L_{sh}$  and  $C_{sh}$  which are due to the change in via positions and resonator positions, respectively. Hence, the change of the resonator tilt angle affects only the total shunt admittance  $Y_{sh}$ . With the increase of tilt angles, the shunt resonance frequency is solely moving toward the desired balanced frequency of 11.5 GHz keeping the series resonance frequency almost stationary. The increment of  $L_{sh}$  with the increment of the resonator tilt angle  $\zeta$  is not significant as the number of vias is not changing. However, the increment of  $C_{sh}$  is more prominent due to the changing position of EMSIW. The increment of  $C_{sh}$  implies the increment of shunt admittance which increases the shunt contribution in radiation mechanism. In the full-wave simulation of the unit cell, wave-port excitation is carried out. By considering the effect of periodicity, the unit cell is simulated in HFSS and the S-parameters are extracted to study the dispersion characteristics. The dispersion equation of the periodic TL can be extracted from full-wave simulations [4], [5]. The dispersion curve of the proposed unit cell in the present situation is obtained by computing  $\beta$  and  $\alpha$  parameters using the following expressions:

$$\beta = \frac{1}{p_1} \left| \text{Im} \left( \cosh^{-1} \left( \frac{1 - S_{11}S_{22} + S_{12}S_{21}}{2S_{21}} \right) \right) \right| \quad (1)$$

$$\alpha = \frac{1}{p_1} \left| \text{Re} \left( \cosh^{-1} \left( \frac{1 - S_{11}S_{22} + S_{12}S_{21}}{2S_{21}} \right) \right) \right| \quad (2)$$

where the HFSS full-wave simulator is employed to estimate the S-parameters of the cell in terms of its geometry at specified

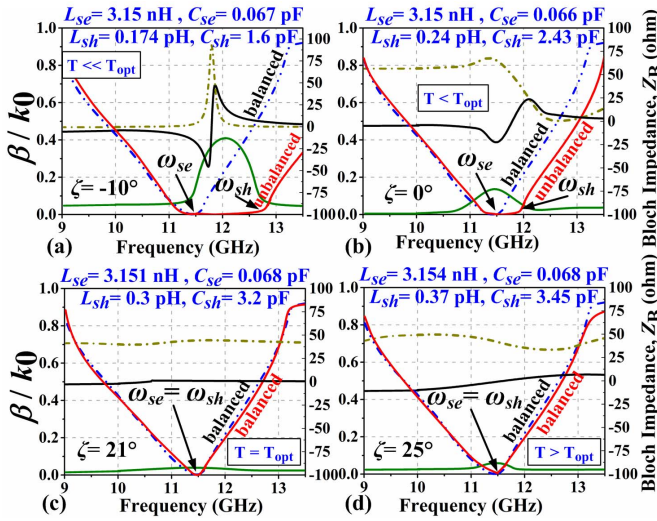


Fig. 4. Variation of  $\zeta$  and its effect on dispersion diagram for (a)  $T < T_{opt}$ , (b)  $T < T_{opt}$ , (c)  $T = T_{opt}$ , and (d)  $T > T_{opt}$ .

frequency points. After estimating  $\beta$  and  $\alpha$  parameters, the dispersion diagram representing the factors  $(|\beta|/k_0)$  and  $(|\alpha|/k_0)$  with  $k_0 = 2\pi f/c$  as a function of frequency  $f$  is plotted as shown in Fig. 2(b). It is observed from the dispersion diagram [Fig. 2(b)] that at the transition frequency ( $f_0 = 11.5$  GHz) where radiated fan-beam is in broadside direction,  $f_{se}$  and  $f_{sh}$  are equal. Thus, the balance condition is achieved. At this condition, phase constant  $\beta$  exhibits zero value at the transition frequency. Below this frequency, the LH region appears which supports the propagation of backward-wave and just above the transition frequency is the RH region which supports forward-wave. After achieving the balanced condition, if we now increase the resonator tilt angle furthermore which signifies the excessive asymmetry, the shunt capacitance further increases and transformation ratio exceeds its optimal value. Generally, the variation of the tilt angle ( $\zeta$ ) is a very easier way to get excessive asymmetry in transverse as well as the longitudinal direction. The proposed asymmetry gradually decreases the shunt  $Q$ -factor to a value of  $\sim 12.72$ , which eventually enhances the shunt radiation contribution. Similarly, the series  $Q$ -factor is also enhanced during this process resulting in the value of 12.73. At this condition,  $\eta_{f_0}$  enhances from off-broadside.  $\eta_{f_0}$  is the overall radiation efficiency at broadside frequency ( $f_0$ ), i.e., 11.5 GHz, and it can be calculated from [14]. The variation of  $\zeta$  and its effect on dispersion diagram and Bloch impedance ( $Z_B$ ) are shown in Fig. 4 where the optimized circuit element values are mentioned for each step. Moreover, one can justify if the tilt angle  $\zeta$  increases, the radiation resistance  $R_{rad}$  also increases because of larger accumulation of charges at the tip of the resonator along with decrements of loss resistance. As a result, overall radiation efficiency increases and after  $\zeta > \zeta_{opt}$  value ( $\zeta = 25^\circ$ ) [Fig. 4(d)], even it is greater than off-broadside because of the excessive shunt coupled power transfer to load as shown below in Fig. 5(a).

### B. Technique 2: Enhancement of $\eta_{f_0}$ by Independent Series Parameter Control Equivalently Varying the Tilt Angle of IDC Slot ( $\theta$ )

The proposed design provides another way to control the transformation ratio, and, hence, to improve the broadside radiation efficiency profile. In this approach, even and odd excitation analyses are carried out in a similar manner as mentioned in the previous approach. For

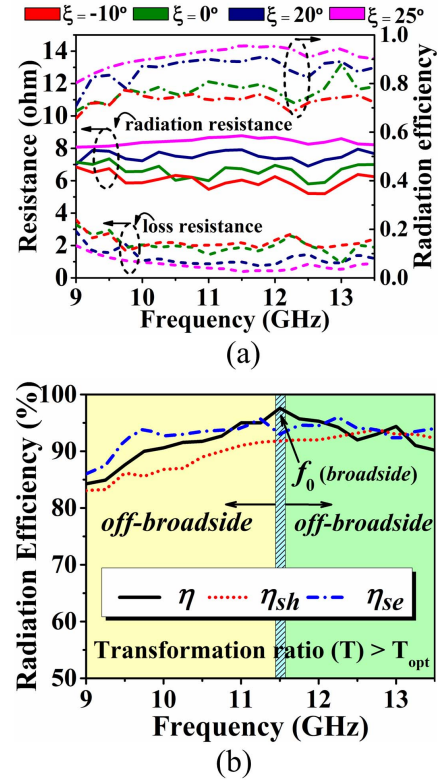


Fig. 5. (a) Variation of EMSIW resonator tilt angle  $\zeta$  and its effect on radiation resistance, loss resistance, and efficiency. (b) Variation of series, shunt, and overall radiation efficiency of the proposed antenna.

this situation, the tilt angle of the IDC slot ( $\theta$ ) is varied. The IDC slot mostly affects the series capacitance  $C_{se}$  but variation of  $\theta$  also changes  $L_{se}$ . When the IDC slot tilt angle  $\theta$  increases gradually, both the series inductance and capacitance are decreased. As a result, the series resonance frequency is moved toward higher value. For the  $\theta$  of  $10^\circ$ , both the series and shunt frequencies are equal and fulfill the balanced condition at 11.5 GHz. At this point, transformation ratio reaches its optimal value ( $T = 1.079$ ), and the  $Q$ -factor for series and shunt resonances is equal and it is obtained as 12.73. Here,  $\eta_{f_0}$  is almost equal to the off-broadside and the series and shunt modes no longer exist because of forming new coupled modes. Now if one increases  $\theta$  more than  $10^\circ$  ( $13^\circ$  for our design purpose), i.e., asymmetry is applied beyond the optimal point,  $C_{se}$  and  $L_{se}$  are also decreased furthermore keeping the dispersion behavior almost unchanged. Thus, series impedance increases with increased  $V_{se}/I_{se}$ . In parallel, due to the simultaneous increment of increased series radiation resistance, the series power ratio is enhanced with the maximum coupling of series power. The above described detailed analysis shows that the overall radiation efficiency at broadside direction ( $\eta_{f_0}$ ) has been increased by controlling the power ratio between the series and the shunt resonators through larger TA. The series and shunt radiation efficiencies are calculated from [14]. The efficiency at broadside frequency ( $\eta_{f_0}$ ) of  $\sim 96\%$  is achieved over off-broadside and is shown in Fig. 5(b).

### III. LEAKY-WAVE ANTENNA DESIGN

The balanced CRLH unit cell shown in Fig. 1(a) is placed periodically in series with the periodicity  $p_1$  (maintaining the homogeneity condition, i.e.,  $p_1 \ll \lambda_g/4$ ) in such a manner that the scanning range of the LWA will be in the fast-wave region (9–13.5 GHz) where



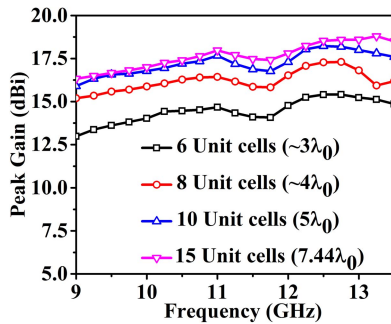


Fig. 6. Selection of compact antenna size by optimizing peak gain variation for different radiator lengths.

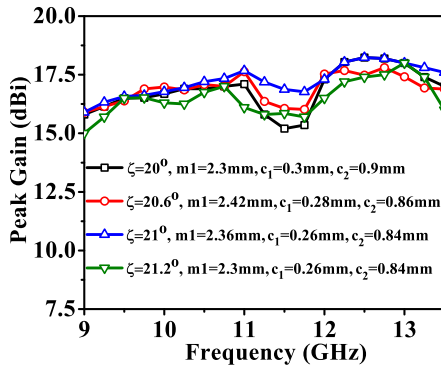


Fig. 7. Gradual optimization for the selection of structural parameters to minimize the gain drop in broadside direction.

$n$ th space harmonic phase constant ( $\beta_n$ ) increases from negative ( $\beta_n = -k_0$ ) to positive ( $\beta_n = k_0$ ) values with increment of frequencies. In the fast-wave region,  $\beta_n$  is less than the free-space wavenumber, i.e.,  $|\beta_n| < k_0$ , which is the necessary radiation condition of LWA. In the proposed design,  $n = 0$  harmonic is responsible for radiation and it is termed as  $\beta$ . According to the Hensen–Woodyard maximum directivity condition [2], the largest directivity of our proposed antenna will occur for the radiator length of 133 mm ( $5\lambda_0$ ) which contains ten unit cells. If we increase the radiator length, i.e., increase the number of unit cells, the gain is increased accordingly but it does not show significant improvement after  $5\lambda_0$ . Little increment is observed due to slight improvement of the radiation efficiency. Selection of compact antenna size by optimizing peak gain variation for different radiator lengths is shown in Fig. 6, from where it is clear that maximum directivity and gain can be achieved with the radiator length of  $5\lambda_0$  keeping the antenna size most compact. It is also observed that the inaccurate dispersion is responsible for gain degradation in broadside direction. In order to minimize the gain drop along the broadside direction, the precise tuning of various structural parameters of the proposed unit cell structure is carried out in the gradual fashion. The optimization results into minimum gain drop around the broadside frequency point as shown by blue line in Fig. 7. The angle of radiation from the  $z$ -axis can be determined from the following equation [21]:

$$\theta_m = \sin^{-1} \left( \frac{|\beta|}{k_0} \right) = \sin^{-1} \left( \frac{|\beta| \cdot c}{2\pi f} \right). \quad (3)$$

#### IV. RESULTS AND DISCUSSION

To validate the proposed design experimentally, the prototype is fabricated on Rogers RT/duroid 5880 substrate having the dielectric loss resulting in larger beamwidth. The measured minimum cross-polarization levels are obtained as  $-22.39$  dB at 9 GHz,  $-24.89$  dB at 10 GHz,  $-20.74$  dB at 11.5 GHz,  $-22.16$  dB at 13 GHz, and

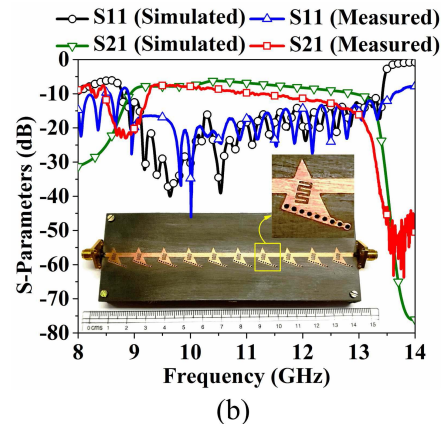
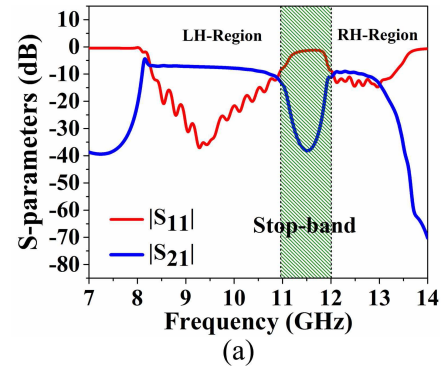


Fig. 8. S-parameter responses of (a) unbalanced CRLH LWA with broadside null and (b) proposed balanced CRLH LWA.

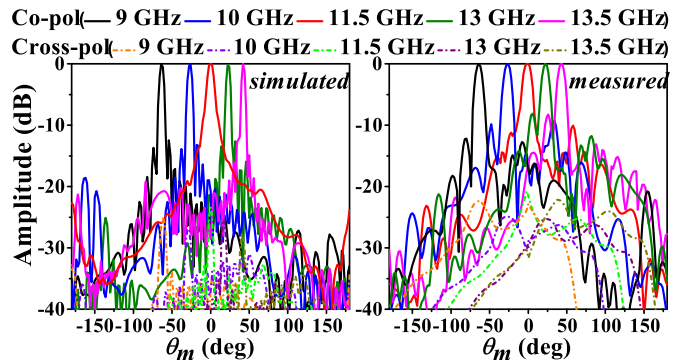


Fig. 9. (a) Simulated and (b) measured radiation patterns of the proposed LWA in  $xz$  plane at 9 GHz ( $\theta_m = -60^\circ$ ), 10 GHz ( $\theta_m = -25^\circ$ ), 11.5 GHz ( $\theta_m = 0^\circ$ ), 13 GHz ( $\theta_m = 23^\circ$ ), and 13.5 GHz ( $\theta_m = 40^\circ$ ).

simulated and measured 10 dB return loss bandwidths [Fig. 8(b)] of the proposed antenna have achieved 40.64% (8.88–13.41 GHz) and 40.89% (8.93–13.52 GHz), respectively. The open stopband, shown in Fig. 8(a) (broadside null at 11.5 GHz), is successfully suppressed and as a result, broadside radiation is obtained. The simulated and measured normalized radiation patterns are shown in Fig. 9(a) and (b) where the measured radiated beam of the proposed antenna scans from the LH region of  $\theta_m = -64^\circ$  at 9 GHz to the RH region of  $\theta_m = 43^\circ$  at 13.5 GHz, including broadside radiation at 11.5 GHz. The measured scanning range is obtained as  $107^\circ$ . Little discrepancy in measured radiation pattern is due to larger leakage loss resulting in larger beamwidth. The measured minimum cross-polarization levels are obtained as  $-22.39$  dB at 9 GHz,  $-24.89$  dB at 10 GHz,  $-20.74$  dB at 11.5 GHz,  $-22.16$  dB at 13 GHz, and

TABLE I  
PERFORMANCE COMPARISON OF PROPOSED STRUCTURE WITH OUR SIMPLE EMSIW-BASED LWA

Unit cell configuration	Length	Deg. of freedom	$\eta_{f_0}$	BW	$G_p$ (dBi)	$\Delta\theta$
Simple EMSIW based LWA	$7.26\lambda_0$ with 10 unit cells	Limited	90.8%; (limited $\eta_{f_0}$ because equalization of $\eta_{se}$ and $\eta_{sh}$ limit $\eta_{f_0}$ up to certain point)	22.22% (8-10 GHz)	13.31 dBi (simple EMSIW has lower radiation intensity)	Only 1 quadrant scanning of $51^\circ$ ( $37^\circ$ to $88^\circ$ )
<b>Proposed DA EMSIW based CRLH LWA with tilted IDC</b>	<b><math>5\lambda_0</math> with 10 unit cells; more compact</b>	<b>Larger</b>	<b>96%; (independent control over <math>\eta_{se}</math> and <math>\eta_{sh}</math> enhance <math>\eta_{f_0}</math> significantly)</b>	<b>40.89% (9-13.5 GHz)</b>	<b>17.96 dBi (high gain and directivity due to larger radiation intensity)</b>	<b>Full space 2 quadrant scanning of <math>107^\circ</math> (<math>-64^\circ</math> to <math>+43^\circ</math>)</b>

TABLE II  
PERFORMANCE COMPARISON WITH OTHER REPORTED DESIGNS

Reference	Length	Bandwidth (%)	$G_p$ (dBi)	$\Delta\theta$	$\eta_{f_0}$
[6] SIW based CRLH LWA	$7\lambda_0$	8.6-12.8 GHz(39.25%)	10.8	$130^\circ$	78%
[7] CRLH based Multilayer LWA	$12.95\lambda_0$	20-30 GHz(40%)	14	$75^\circ$	54%
[9] HMSIW based CRLH LWA	$4.85\lambda_0$	13.5-17.8 GHz(27.47%)	16	$86^\circ$	83%
[12] HMSIW based LWA	$6.6\lambda_0$	9-13.5 GHz(30.3%)	10	$86^\circ$	64%
[13] Series-fed patch based TA P-LWA	$27\lambda_0$	9-11 GHz(20%)	NA	NA	69%
[14] Series-fed patch based DA P-LWA	$\sim 5\lambda_0$	22-26 GHz(16.6%)	8.5	NA	86%
EMSIW based LWA without IDC	$\sim 5.2\lambda_0$	8-10 GHz(22.22%)	13.31	$51^\circ$	84%
<b>Proposed: EMSIW based CRLH DA LWA</b>	<b><math>5\lambda_0</math></b>	<b>9-13.5 GHz(40.89%)</b>	<b>17.96</b>	<b><math>107^\circ</math></b>	<b>96%</b>

$\eta_{f_0}$  = radiation efficiency at broadside frequency.

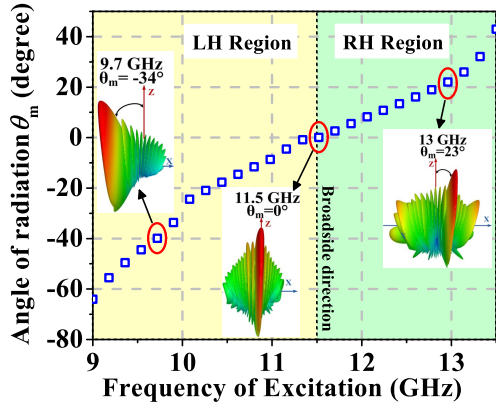


Fig. 10. Variation of angle of radiation with excitation frequency (3-D patterns are in inset for three different frequencies).





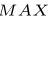
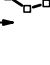

$-25.29$  dB at 13.5 GHz. Now, in order to estimate the angle of radiation ( $\theta_m$ ) as a function of frequency using (3), the phase constant ( $\beta$ ) in terms of S-parameters of the corresponding unit cell along with its periodic length ( $p_1$ ) is obtained using the data given in Fig. 2(b). Once the factor ( $|\beta|/k_0$ ) is determined using the data given in Fig. 2(b), the curve showing the plot of the angle of radiation  $\theta_m$  (in the vertical axis) versus the corresponding frequency of excitation “ $f$ ” (in the horizontal axis) can be obtained using (3) as shown in Fig. 10. Fig. 11 demonstrates that the peak gain ( $G_p$ ) and overall radiation efficiency values obtained from simulation and measurement are in good agreement. In order to show the advantages of the proposed antenna, a detailed comparison is made with our own simple EMSIW-based structure as well as with similar types of structures proposed in the literature as shown in Tables I and II, respectively. The proposed prototype appears to be a much better alternative as compared to the simple EMSIW-based LWA to facilitate wider scanning range, higher gain, and larger radiation efficiency with much compact geometry. Due to the incorporation of suitably tilted IDC slot on tilted EMSIW, not only larger degrees of freedom is achieved to independently control series and shunt parameters but also increase in the radiation intensity results in significant gain enhancement and

compactness. It can clearly be seen from Table II that the proposed antenna is advantageous in terms of high gain, enhanced efficiency at broadside frequency with additional degrees of freedom, compact size, and good operating bandwidth along with suitable scanning range than other reported designs. It is to be noted that, [6], [7], [9], [12], and [13] have considerably low  $\eta_{f_0}$  due to either double symmetry or single asymmetry. Although [14] has DA with comparable size and, therefore, increased  $\eta_{f_0}$ , it suffers lower  $G_p$  (8.5 dBi), inadequate bandwidth (16.6%), lesser radiation efficiency (86%) at broadside frequency, and higher cross-polar level of  $-13.75$  dB compared to the proposed design. To analyze the proposed LWA performance rigorously, the proposed structure with optimized IDC configuration is compared with the earlier reported CRLH-based IDC loaded LWA structures as shown in Table III. In Table III, although [16] and [20] have almost comparable radiator lengths, the proposed structure is advantageous in terms of higher gain, larger radiation efficiency, and working bandwidth. It should be noted that although the work proposed in [6] and [18] of Table III provides larger scanning ranges along with comparable operating bandwidth, the proposed structure is advantageous due to its higher gain, much compact dimension, and larger radiation efficiency.

## V. CONCLUSION

A simple high gain larger full space scanning range compact LWA based on the use of DA CRLH unit cell has been demonstrated. The proposed structure makes use of the tilted radiating EMSIW incorporated with IDC slot to realize CRLH media, which enhances the radiation intensity profile of the unit cell significantly resulting in higher directivity and gain keeping the proposed prototype quite compact. Maintaining the frequency balanced condition of our proposed unit cell, the propagation constant and Bloch impedance of the series and shunt resonators can be independently controlled for easier tuning of transformation ratio to obtain larger efficiency at broadside frequency over off-broadside and it achieved  $\sim 96\%$ . The proposed antenna shows a fair scanning range of  $107^\circ$  ( $-64^\circ - +43^\circ$ ) with a high gain of 17.96 dBi. The measured results are in well accordance with experiments which prove the effectiveness and validity of the

TABLE III  
PERFORMANCE COMPARISON WITH OTHER IDC SLOT BASED REPORTED DESIGNS

Design of CRLH based LWAs with IDC unit cell	Radiator length	Bandwidth(%)	$G_p$ (dBi)	$\Delta\theta$	$\eta_{MAX}$
[6] SIW based CRLH LWA with IDC slots 	$7\lambda_0$	8.6-12.8 GHz(39.25%)	10.8	$130^\circ$ ( $-70^\circ$ to $+60^\circ$ )	78%
[16] SI CRLH LWA with orthogonal IDC pair 	$5.6\lambda_0$	7.5-10 GHz(25.57%)	12	$80^\circ$ ( $-30^\circ$ to $+40^\circ$ )	80%
[17] IDC loaded HMSIW based LWA 	$3.25\lambda_0$	Fixed freq. beam scanning	$\sim 10$	$67^\circ$ ( $-31^\circ$ to $+35^\circ$ )	NA
[18] HMSIW based LWA with ramp-shaped IDC 	$6.2\lambda_0$	7.4-13.5 GHz(54%)	12.01	$140^\circ$ ( $-70^\circ$ to $+70^\circ$ )	NA
[19] SIW based CRLH LWA with $\pm 45^\circ$ tilted IDC 	$2.42\lambda_0$	4.2-4.85 GHz(14.36%)	2.5	$51^\circ$ ( $-25^\circ$ to $+26^\circ$ )	NA
[20] SIW based CRLH LWA with T-shaped IDC pair 	$5.6\lambda_0$	7.15-10.35 GHz(36.57%)	8.95	$103^\circ$ ( $-19^\circ$ to $+84^\circ$ )	69%
<b>Proposed: EMSIW based CRLH LWA with tilted IDC</b> 	$5\lambda_0$	<b>9-13.5 GHz(40.89%)</b>	<b>17.96</b>	<b><math>107^\circ</math> (<math>-64^\circ</math> to <math>+43^\circ</math>)</b>	<b>96%</b>

$G_p$  = Peak gain,  $\Delta\theta$  = Scanning range,  $\eta_{MAX}$  = maximum radiation efficiency.

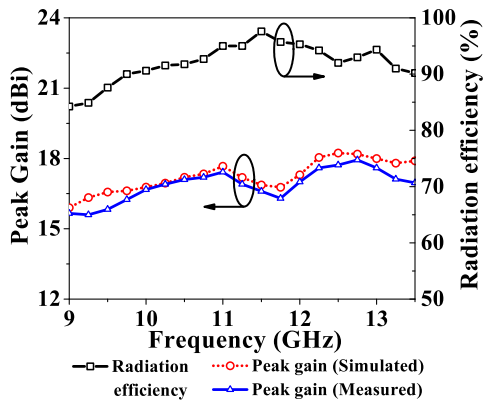


Fig. 11. Variation of peak gain and overall radiation efficiency with frequency.

proposed design. Having the advantages of more degrees of freedom to achieve larger efficiency, simple design methodology, being compact, adequate gain, and larger scanning range, the proposed antenna could be the potential candidate for several frequency beam scanning applications.

REFERENCES

[1] C. Caloz and T. Itoh, *Electromagnetic Metamaterials: Transmission Line Theory and Microwave Applications*. Hoboken, NJ, USA: Wiley, 2005.  
 [2] D. R. Jackson and A. A. Oliner, "Leaky-wave antennas," in *Modern Antenna Handbook*, C. A. Balanis, Ed. Hoboken, NJ, USA: Wiley.  
 [3] S.-T. Yang and H. Ling, "Two-section half-width microstrip leaky wave antenna," *IEEE Trans. Antennas Propag.*, vol. 62, no. 10, pp. 4988–4996, Oct. 2014.  
 [4] J. Liu, D. R. Jackson, and Y. Long, "Substrate integrated waveguide (SIW) leaky-wave antenna with transverse slots," *IEEE Trans. Antennas Propag.*, vol. 60, no. 1, pp. 20–29, Jan. 2012.  
 [5] A. Sarkar, A. Sharma, M. Adhikary, A. Biswas, and M. J. Akhtar, "Bi-directional SIW leaky-wave antenna using TE<sub>20</sub> mode for frequency beam scanning," *Electron. Lett.*, vol. 53, no. 15, pp. 1017–1019, Jul. 2017.  
 [6] Y. D. Dong and T. Itoh, "Composite right/left-handed substrate integrated waveguide and half mode substrate integrated waveguide leaky-wave structures," *IEEE Trans. Antennas Propag.*, vol. 59, no. 3, pp. 767–775, Mar. 2011.  
 [7] W. Jiang, C. Liu, B. Zhang, and W. Menzel, "K-band frequency-scanned leaky-wave antenna based on composite right/left-handed transmission lines," *IEEE Antennas Wireless Propag. Lett.*, vol. 12, pp. 1133–1136, 2013.

[8] J. Xu, W. Hong, H. Tang, Z. Kuai, and K. Wu, "Half-mode substrate integrated waveguide (HMSIW) leaky-wave antenna for millimeter-wave applications," *IEEE Antennas Wireless Propag. Lett.*, vol. 7, pp. 85–88, 2008.  
 [9] A. Sarkar, M. Adhikary, A. Sharma, A. Biswas, M. J. Akhtar, and Z. R. Hu, "Composite right/left-handed based compact and high gain leaky-wave antenna using complementary spiral resonator on HMSIW for Ku band applications," *IET Microw. Antennas Propag.*, vol. 12, no. 8, pp. 1310–1315, Jun. 2018.  
 [10] D. Lee and S. Lim, "Leaky-wave antenna design using quarter-mode substrate-integrated waveguide," *Microw. Opt. Technol. Lett.*, vol. 57, May 2015, pp. 1234–1236.  
 [11] M. U. Memon and S. Lim, "Frequency-tunable compact antenna using quarter-mode substrate integrated waveguide," *IEEE Antennas Wireless Propag. Lett.*, vol. 14, pp. 1606–1609, 2015.  
 [12] R. Henry and M. Okoniewski, "A broadside-scanning half-mode substrate integrated waveguide periodic leaky-wave antenna," *IEEE Antennas Wireless Propag. Lett.*, vol. 13, pp. 1429–1432, 2014.  
 [13] S. Otto, A. Al-Bassam, A. Rennings, K. Solbach, and C. Caloz, "Transversal asymmetry in periodic leaky-wave antennas for bloch impedance and radiation efficiency equalization through broadside," *IEEE Trans. Antennas Propag.*, vol. 62, no. 10, pp. 5037–5054, Oct. 2014.  
 [14] A. Al-Bassam, S. Otto, D. Heberling, and C. Caloz, "Broadside dual-channel orthogonal-polarization radiation using a double-asymmetric periodic leaky-wave antenna," *IEEE Trans. Antennas Propag.*, vol. 65, no. 6, pp. 2855–2864, Jun. 2017.  
 [15] S. Sam and S. Lim, "Electrically small eighth-mode substrate-integrated waveguide (EMSIW) antenna with different resonant frequencies depending on rotation of complementary split ring resonator," *IEEE Trans. Antennas Propag.*, vol. 61, no. 10, pp. 4933–4939, Oct. 2013.  
 [16] Y. Dong and T. Itoh, "Substrate integrated composite right-/left-handed leaky-wave structure for polarization-flexible antenna application," *IEEE Trans. Antennas Propag.*, vol. 60, no. 2, pp. 760–771, Feb. 2012.  
 [17] A. Suintives and S. V. Hum, "A fixed-frequency beam-steerable half-mode substrate integrated waveguide leaky-wave antenna," *IEEE Trans. Antennas Propag.*, vol. 60, no. 5, pp. 2540–2544, May 2012.  
 [18] A. P. Saghati, M. M. Mirsalehi, and M. H. Neshati, "A HMSIW circularly polarized leaky-wave antenna with backward, broadside, and forward radiation," *IEEE Antennas Wireless Propag. Lett.*, vol. 13, pp. 451–454, 2014.  
 [19] H. Lee, J. H. Choi, C.-T. M. Wu, and T. Itoh, "A compact single radiator CRLH-inspired circularly polarized leaky-wave antenna based on substrate-integrated waveguide," *IEEE Trans. Antennas Propag.*, vol. 63, no. 10, pp. 4566–4572, Oct. 2015.  
 [20] M. M. Sabahi, A. A. Heidari, and M. Movahhedi, "A compact CRLH circularly polarized leaky-wave antenna based on substrate-integrated waveguide," *IEEE Trans. Antennas Propag.*, vol. 66, no. 9, pp. 4407–4414, Sep. 2018.  
 [21] C. A. Balanis, *Modern Antenna Handbook*. Hoboken, NJ, USA: Wiley, 2008.